THE JOURNAL OF BIOLOGICAL CHEMISTRY VOL. 286, NO. 31, pp. 27559–27572, August 5, 2011

Suppression of Amyloid β A11 Antibody Immunoreactivity by Vitamin C

POSSIBLE ROLE OF HEPARAN SULFATE OLIGOSACCHARIDES DERIVED FROM GLYPICAN-1 BY ASCORBATE-INDUCED, NITRIC OXIDE (NO)-CATALYZED DEGRADATION[*][S]

Received for publication, March 24, 2011, and in revised form, May 13, 2011 Published, JBC Papers in Press, June 3, 2011, DOI 10.1074/jbc.M111.243345

Fang Cheng[‡], Roberto Cappai[§¶], Giuseppe D. Ciccotosto[§¶], Gabriel Svensson[‡], Gerd Multhaup[‖], Lars-Åke Fransson[‡1], and Katrin Mani[‡2]

From the [‡]Department of Experimental Medical Science, Division of Neuroscience, Glycobiology Group, Lund University, Biomedical Center A13, SE-221 84 Lund, Sweden, [§]Department of Pathology and [¶]Bio21 Molecular Science and Biotechnology Institute, The University of Melbourne, Victoria 3010, Australia, and [‖]Institute for Chemistry/Biochemistry, Free University of Berlin, Thielallee 63, D-14195 Berlin, Germany

Amyloid β (Aβ) is generated from the copper- and heparan sulfate (HS)-binding amyloid precursor protein (APP) by proteolytic processing. APP supports *S*-nitrosylation of the HS proteoglycan glypican-1 (Gpc-1). In the presence of ascorbate, there is NO-catalyzed release of anhydromannose (anMan)-containing oligosaccharides from Gpc-1-nitrosothiol. We investigated whether these oligosaccharides interact with Aβ during APP processing and plaque formation. anMan immunoreactivity was detected in amyloid plaques of Alzheimer (AD) and APP transgenic (Tg2576) mouse brains by immunofluorescence microscopy. APP/APP degradation products detected by antibodies to the C terminus of APP, but not Aβ oligomers detected by the anti-Aβ A11 antibody, colocalized with anMan immunoreactivity in Tg2576 fibroblasts. A 50–55-kDa anionic, sodium dodecyl sulfate-stable, anMan- and Aβ-immunoreactive species was obtained from Tg2576 fibroblasts using immunoprecipitation with anti-APP (C terminus). anMan-containing HS oligo- and disaccharide preparations modulated or suppressed A11 immunoreactivity and oligomerization of Aβ42 peptide in an *in vitro* assay. A11 immunoreactivity increased in Tg2576 fibroblasts when Gpc-1 autoprocessing was inhibited by 3-β[2(diethylamino)ethoxy]androst-5-en-17-one (U18666A) and decreased when Gpc-1 autoprocessing was stimulated by ascorbate. Neither overexpression of Gpc-1 in Tg2576 fibroblasts nor addition of copper ion and NO donor to hippocampal slices from 3xTg-AD mice affected A11 immunoreactivity levels. However, A11 immunoreactivity was greatly suppressed by the subsequent addition of ascorbate. We speculate that temporary interaction between the Aβ domain and small, anMan-containing oligosaccharides may preclude formation of toxic Aβ oligomers. A portion of the oligosaccharides are co-secreted with the Aβ peptides and deposited in plaques. These results support the notion that an inadequate supply of vitamin C could contribute to late onset AD in humans.

The amyloid β (Aβ)[3] peptides that have a central role in Alzheimer disease (AD) are derived from the amyloid precursor protein (APP). APP is a copper- and heparan sulfate (HS)-binding membrane protein, which is expressed in many cell types, including neural cells and fibroblasts (1–4). Processing of APP involves several proteases and regulatory proteins, collectively designated α-, β-, and γ-secretases (supplemental Fig. S1, a–c). Single α- or β-cleavages result in the release of the large ectodomain, whereas the C-terminal fragments (APP-CTF-α and APP-CTF-β, respectively) remain tethered to the membrane. Combined β- and γ-cleavages are amyloidogenic and lead to release of the C-terminal cytoplasmic domain of APP and the generation of Aβ peptides, mostly Aβ40 and Aβ42. Aβ peptides first form soluble oligomers and then insoluble aggregates that accumulate as amyloid fibrils and senile plaques in the brain of AD patients. Soluble Aβ oligomers formed at early stages of AD are believed to be particularly toxic and responsible for early memory failure (5–9).

Cell surface-located APP can be associated with lipid rafts and processed via β-cleavage during caveolar endocytosis (10–14). Aβ peptides are formed upon subsequent γ-cleavage inside neurons and are then secreted (7). Transgenic AD mouse models, such as Tg2576 and 3xTg-AD, overproduce Aβ peptides that oligomerize in late endosomes of neurons (15–18). Some of these toxic prefibrillar Aβ oligomers can be detected with the

* This work was supported by grants from the Swedish Science Council (VR-M); the Bergvall, Crafoord, Hedborg, Kock, Segerfalk, Zoega, and Österlund Foundations; and the Medical Faculty of Lund University (to L.-Å. F. and K. M.) and in part by the National Health and Medical Research Council of Australia (to R. C.) and the Deutsche Forschungsgemeinschaft (to G. M.).

[S] The on-line version of this article (available at http://www.jbc.org) contains supplemental Figs. S1–S3 and Table 1.

[1] To whom correspondence may be addressed: Dept. of Experimental Medical Science, Division of Neuroscience, Glycobiology Group, Lund University, BMC A13, SE-221 84 Lund, Sweden. Tel.: 46-46-222-8573; Fax: 46-46-222-0615; E-mail: Lars-Ake.Fransson@med.lu.se.

[2] To whom correspondence may be addressed: Dept. of Experimental Medical Science, Division of Neuroscience, Glycobiology Group, Lund University, BMC A13, SE-221 84 Lund, Sweden. Tel.: 46-46-222-4077; Fax: 46-46-222-0615; E-mail: katrin.mani@med.lu.se.

[3] The abbreviations used are: Aβ, amyloid β; anMan, anhydromannose; AD, Alzheimer disease; APP, amyloid precursor protein; APP-CTF-α, C-terminal α-secretase cleavage product of APP; APP-CTF-β, C-terminal β-secretase cleavage product of APP; Gpc-1, glypican-1; $GlcNH_3^+$, *N*-unsubstituted glucosamine; HS, heparan sulfate; SNO, nitrosothiol; Tg, transgene; U18666A, 3-β[2(diethylamino)ethoxy]androst-5-en-17-one; Tricine, *N*-[2-hydroxy-1,1-bis(hydroxymethyl)ethyl]glycine; RIPA, radioimmune precipitation assay; Bis-Tris, 2-[bis(2-hydroxyethyl)amino]-2-(hydroxymethyl)propane-1,3-diol; OligoII, HS oligosaccharides.

polyclonal antibody A11, which appears to recognize a particular conformation (8, 18).

β-Secretase cleavage occurs in early endosomes, and γ-cleavage can occur in multivesicular late endosomes where Aβ peptides associate with intraluminal vesicles, which can be secreted as exosomes (16, 19, 20). When γ-cleavage is inhibited, exosomes contain increased amounts of APP-CTF-β (20, 21).

The role of glycosaminoglycans, such as HS, in APP processing and amyloid formation is not fully understood. Although intact HS chains can change protein conformations into amyloidogenic forms, small HS oligosaccharides are without effect (22). HS degradation products may even inhibit amyloid formation as overexpression of heparanase affords protection against amyloidosis (23). Aβ amyloid deposits contain HS and HS proteoglycans (24–28). The origin of amyloid-associated HS is unclear, but some of the HS co-deposited with extracellular Aβ in both sporadic and familial AD as well as in Tg2576 mice can be derived from the HS proteoglycans glypican-1 (Gpc-1) and syndecan-3 produced by glial cells (29).

APP interacts strongly with Gpc-1 (30), a major glypican isoform in the adult brain (31). Gpc-1, which is synthesized by both neural and glial cells, has a glycosylphosphatidylinositol anchor that localizes to lipid rafts where Gpc-1 can interact with Aβ (14). Gpc-1 can also be internalized and recycled via a caveolin-1-associated endosomal route where it is subjected to modification and processing (32). First, cysteines in the Gpc-1 core protein are *S*-nitrosylated (nitric oxide (NO) is added) by endogenously formed nitric oxide (NO) in a Cu(II)-dependent redox reaction (33–35). Free copper ions are scarce *in vivo*, but Cu(II)-loaded cuproproteins, such as the glycosylphosphatidylinositol-anchored ceruloplasmin (36) and prion proteins (34, 37) as well as APP, can support *S*-nitrosylation of Gpc-1. Moreover, APP and Gpc-1 colocalize in subcellular compartments of neuroblastoma cells (38).

Second, during endosomal transport, Gpc-1-SNO undergoes NO-dependent deaminative cleavage of its HS chains (supplemental Fig. S1d). This is induced by an unknown reducing agent (39) and probably catalyzed by nitroxyl (HNO) derived from the intrinsic SNO groups (33, 40, 41). Cleavage of the HS chains occurs at the relatively rare *N*-unsubstituted glucosamine ($GlcNH_3^+$) sites. During cleavage, $GlcNH_3^+$ is converted to anhydromannose (anMan), which becomes the reducing terminal sugar of the released HS degradation products. These products accumulate in Rab7-positive late endosomes (41). NO release and subsequent deaminative cleavage of HS can also be induced by exogenously supplied vitamin C in the ascorbate or dehydroascorbate form, depending on the cell type (40, 41).

The reducing terminal anMan residue in the released HS degradation products contains a free aldehyde that can form an unstable aldimine bond to amino groups in proteins, *i.e.* a Schiff base. A stable covalent bond could then be formed by reduction or rearrangement (supplemental Fig. S1e and Refs. 31 and 42). Covalent conjugates between anMan-containing HS oligosaccharides and proteins have been found in T24 carcinoma and N2a neuroblastoma cells (43).

Because APP interacts with Gpc-1 and modulates the copper- and NO-dependent release of HS from Gpc-1 both *in vitro* and *in vivo* (38), we decided to investigate whether anMan-containing HS degradation products generated by Gpc-1 autoprocessing interact with APP degradation products and whether such HS is ultimately deposited in amyloid plaques. For this purpose, we examined normal human and AD brains as well as brains and/or fibroblasts from wild-type, Tg2576, and 3xTg-AD mice for anMan- and Aβ-immunoreactive components. We show here that anMan immunoreactivity is present in amyloid plaques from human AD and Tg2576 mouse brains. In extracts of fibroblasts from Tg2576 mice, we found that anMan immunoreactivity co-precipitated with APP-CTF-β, yielding a 50–55-kDa, Aβ(4G8)-immunoreactive, sodium dodecyl sulfate (SDS)-stable species. After radiolabeling with $^{35}SO_4$, an anionic pool comprising both [^{35}S]HS and 70–75-kDa Aβ(4G8)-immunoreactive species was obtained. The addition of anMan-containing HS oligo- or disaccharides to Aβ42 peptide monomers modulated or suppressed the transient appearance of A11 immunoreactivity and inhibited Aβ42 oligomerization. Aβ A11 immunoreactivity in Tg2576 fibroblasts increased when NO-dependent cleavage of HS in Gpc-1 was suppressed. Conversely, when such cleavage was initiated by ascorbate in copper- and NO-supplemented Tg2576 fibroblasts or hippocampal slices from 3xTg-AD mice, A11 immunoreactivity was nearly eliminated.

EXPERIMENTAL PROCEDURES

Materials—Tg2576 mice have been described (44). Triple transgenic AD mice (3xTg-AD) were a kind gift from Professor Mark P. Mattson, Laboratory of Neurosciences, National Institute of Aging Intramural Research Program, Baltimore, MD (17). Brain tissue from non-demented controls and AD patients was obtained from the Victorian Brain Bank Network. Embryonic fibroblasts from wild-type and Tg2576 mice were prepared and maintained as described elsewhere (38). Synthetic Aβ42 was purchased from Millipore. An HS preparation (HS6) with an *N*-sulfate-to-hexosamine molar ratio of 0.72 was obtained as described elsewhere (45) and *N*-desulfated by solvolysis in 5% water, dimethyl sulfoxide (46). anMan-containing HS oligo- and disaccharides were generated by treating the *N*-desulfated HS with HNO_2 at pH 3.9 (35, 47). The extent of degradation was monitored by oligosaccharide PAGE (48). A polyclonal antibody against the APP C terminus (A8717) was from Sigma, polyclonal anti-Aβ (H-43) was from Santa Cruz Biotechnology, polyclonal anti-Aβ oligomer (A11) was from Chemicon, and anti-Aβ17–24 mAb (4G8) was from BioSource. LysoTracker Red; rabbit polyclonal antibodies against Gpc-1 and Rab7; an mAb recognizing anMan-terminating HS oligosaccharides (mAb AM); suitably tagged secondary anti-rabbit, anti-mouse, and anti-goat antibodies; proteinase K, 3-β-[2-(diethylamino)-ethoxy]androst-5-en-17-one (U18666A); and ascorbate were generated/obtained as described previously (32–34, 36, 38, 40, 41, 43, 49). Thioflavin S and proteinase K were purchased from Sigma-Aldrich. All restriction enzymes used were from MBI Fermentas GmbH, and *Taq* polymerase was obtained from Roche Applied Science. The BCA protein assay kit was purchased from Pierce. Novex Tricine gels were from Invitrogen, and protein A-Sepharose CL-4B was from Amersham Biosciences. The ECL Western blotting detection system was from GE Healthcare.

siRNA Preparation and Transfection—The vector pRNA-U6.1/Neo containing the sequence GTTGGTCTACTGTGCTCAT (corresponding to nucleotides 753–771 in mouse Gpc-1) followed by the hairpin sequence TTCAAGAGA, then the reversed complementary Gpc-1 sequence with an additional C in the 5′-end, and a stretch of six T for RNA polymerase III termination followed by GGAA in the 3′-end was synthesized by Genscript Corp. A negative control vector comprising a scrambled sequence was also prepared. Transfection was accomplished by using Lipofectamine (Invitrogen) according to the description of the manufacturer.

Ectopic Expression of Green Fluorescent Protein (GFP)-tagged Gpc-1—The Clontech vector pEGFP C1 was used to create a GFP-Gpc-1 vector. The sequence coding for the N-terminal signal peptide was amplified from cDNA by PCR. The PCR product was digested with AgeI/NheI and ligated into AgeI/NheI-digested pEGFP C1. A Kozak sequence was also introduced with the forward primer. The sequence coding for the core protein and C-terminal signal peptide was also amplified by PCR. The PCR product was digested with HindIII/EcoRI and ligated into HindIII/EcoRI-digested pEGFP C1. The start codon present in the sequence for enhanced GFP was disrupted by using site-directed mutagenesis. The primers used are given in supplemental Table 1. All mutations and constructs were verified by sequencing at Eurofins MWG Operon (Ebersberg, Germany).

The cells were transiently transfected with the vector containing GFP-Gpc-1 for 72 h using Invitrogen's standard protocol for transfection with Lipofectamine 2000. The amount of expression was assessed by immunofluorescence microscopy.

Preparation of Human Brain Tissue, Thioflavin S Staining, and Immunostaining—Formalin-fixed, paraffin-embedded sections from the frontal cortex of post-mortem human brains from non-demented controls and patients with AD were used. Forty-micrometer sections were deparaffinized for immunohistochemistry by standard methods. Sections were then permeabilized in 0.5% Triton X-100, 3% H_2O_2 in phosphate-buffered saline (PBS) for 5 min and then precoated with 10% antimouse total Ig for 1 h at 20 °C. Immunohistochemical staining was performed using overnight treatment with mAb AM at 4 °C followed by treatment with Texas Red-labeled goat antimouse total Ig secondary antibody for 1 h at 20 °C. Controls lacking primary antibody were performed in parallel for all experiments. The thioflavin S staining was then performed as described by Bussière *et al.* (50). Briefly, sections were postfixed in 10% formalin for 10 min and then washed in PBS. After incubation for 10 min in 0.25% potassium permanganate, sections were washed in PBS and incubated in 2% potassium metabisulfite, 1% oxalic acid until they turned white. Sections were then washed in water and stained for 10 min with a solution of 0.015% thioflavin S in 50% ethanol. Finally, sections were washed in 50% ethanol and in water, then dried, and dipped into Histo-Clear before being coverslipped with Permount.

Preparation of Brain Slices and Immunostaining—Animals were kept under pathogen-free conditions in the animal barrier facility at the Biomedical Centre, Lund University, according to the Swedish guidelines for humane treatment of laboratory animals. The experimental setup was approved by the ethics committee for animal research in Malmö/Lund, Sweden. Hippocampal organotypic tissue cultures were prepared as described previously (51). Hippocampi were retrieved from 15-month-old 3xTg-AD mice and cut into 250-μm-thick slices on a MacIllwain tissue chopper. Floating sections from hippocampus were maintained in a culture medium containing minimal essential medium supplemented with 50% horse serum, 2 mM glutamine, 100 units/ml penicillin G, 100 g/ml streptomycin, 0.25% glucose, 0.8% sucrose, and 2% B-27 in a CO_2 incubator at 35 °C for 1 day. Floating sections were then treated with different drugs, and after treatments, the sections were washed with PBS and fixed in 4% paraformaldehyde for 30 min. The endogenous peroxidase activity was quenched for 30 min in 3% H_2O_2. Sections were then incubated in 90% formic acid for 7 min to expose the epitopes. The appropriate primary antibody was applied overnight at 4 °C. Sections were washed with PBS and incubated with the appropriate secondary antibody for 1 h at 20 °C.

Immunofluorescence Microscopy—The various procedures, including the seeding of cells, fixation, use of primary and secondary antibodies, generation of images by sequential scans, and data processing, were the same as those used previously (32–34, 38, 49) or as recommended by the manufacturers. Cells were first precoated with 10% antimouse total Ig and 1% goat serum and then exposed to primary antibodies. The secondary antibody used was either goat anti-mouse total Ig when the primary antibody was monoclonal or goat anti-rabbit IgG when the primary antibody was polyclonal. The secondary antibodies were tagged with either fluorescein isothiocyanate or Texas Red and appropriately combined for colocalization studies. In general, the former tag (green) was used for mAbs, and the latter tag (red) was used for polyclonal antibodies except in combination with LysoTracker Red (red). In the controls, the primary antibody was omitted. The fluorescent images were analyzed using a Carl Zeiss AxioObserver inverted fluorescence microscope equipped with objective EC "Plan-Neofluar" 63×/1.25 oil M27 and AxioCam MRm Rev camera. Identical exposure settings and times were used for image capture when wild-type and Tg2576 cells or untreated and treated cells or tissues were compared.

Flow Cytometry—Cells were seeded in 24-well plates and grown in minimal essential medium containing glutamine, penicillin, streptomycin, and 10% fetal calf serum. Cells were rinsed with medium and detached using trypsin (0.5 ml of 0.05% (w/v) trypsin in PBS for 1 min). Trypsinization was terminated by replacing the trypsin solution with 0.5 ml of medium supplemented with 10% fetal bovine serum. Cells were recovered by gentle suspension and transferred to tubes, adding 1 volume of PBS containing 1% BSA (w/v). Cells were then pelleted by centrifugation and resuspended in 0.2 ml of PBS after removal of the supernatant. Cells were fixed for 30 min in 1 ml of PBS containing 4% paraformaldehyde (w/v) while initially vortexing. Permeabilization was performed by incubation with 0.2% Triton X-100 in PBS (v/v) for 20 min. Immunostaining of the cells was performed as described for immunofluorescence microscopy. In the controls, the primary antibody was omitted. After each step, cells were recovered by centrifugation at 350 × *g* for 5 min. The cells (n = 5,000–10,000) were

finally suspended in PBS containing 1% BSA and analyzed for fluorescence in a fluorescence-assisted cell sorting (FACS) instrument (FACSCalibur, BD Biosciences) operated by CellQuest software. Background fluorescence intensity obtained by omitting the primary antibody was subtracted.

Isolation and Characterization of HS·Protein Complexes—Fibroblasts were incubated with 50 μCi/ml [^{35}S]sulfate for 48 h prior to confluence or kept unlabeled as described elsewhere (43, 47). Cells were lysed by homogenization in RIPA buffer, *i.e.* 0.1% (w/v) SDS, 0.5% (v/v) Triton X-100, 0.5% (w/v) sodium deoxycholate in PBS supplemented with 0.5 mM phenylmethylsulfonyl fluoride at 4 °C. Immunoisolation of APP and APP-derived degradation products from unlabeled cells was performed by using anti-Aβ or anti-APP-CTF polyclonal antibodies followed by adsorption on protein A-Sepharose CL-4B (100 μg of protein A was swelled and used for 1-ml samples containing 1 mg/ml protein). In the controls, no antibody was added. Recovered immunoisolates were displaced by using SDS, and SDS-PAGE was performed on 10% Tricine gels under reducing conditions followed by transfer to PVDF membranes. After coating with unconjugated secondary antibody (1:50), Western blotting was performed by using anMan- or Aβ-specific mAbs as primary antibodies followed by visualization using horseradish peroxidase-conjugated goat anti-mouse IgG as the secondary antibody (1:1000) and developed by ECL chemiluminescence according to the manufacturer's instructions (GE Healthcare) using a Fujifilm ECL detector. In the controls, the primary antibody was omitted. For more details, see legends to the appropriate figures.

Polyanionic compounds were isolated by passing RIPA extracts of cells through DE53 DEAE-cellulose columns (0.2 ml). After extensive rinsing with RIPA buffer, bound anionic material was displaced with 3 × 0.2 ml of 1 M NaCl in the case of unlabeled cells or 4 M guanidinium chloride in the case of [^{35}S]sulfate-labeled cells. Unlabeled eluates were subjected to immunoprecipitation after dialysis against water by spinning in Centricon 30 tubes followed by SDS-PAGE and Western blotting as above. Labeled eluates were subjected to gel exclusion chromatography on Superose 6 or Superdex peptide columns in 4 M guanidinium chloride. Pooled fractions were analyzed by SDS-PAGE and Western blotting as described above. Degradations were performed with proteinase K at a final concentration of 100 μg/ml for 24 h at 56 °C in buffer containing 50 mM Tris/HCl, 5 mM $CaCl_2$, pH 7.5, 0.25% SDS, and 0.25% Triton X-100 or by HS lyase, heparin lyase, or HNO_2 at pH 1.5 or 3.9 as described earlier (43, 47).

In Vitro Assay of Aβ42 A11 Immunoreactivity—The conversion of monomeric Aβ42 to A11-positive soluble oligomers can be monitored by *in vitro* assays (52, 53). We adopted the latter procedure. Aβ42 (21 μg) was first dissolved in 20 μl of hexaisofluoropropanol that was evaporated overnight. Aβ42 was then dissolved in 20 μl of 50 mM NaOH for 30 min, sonicated for 30 min, diluted in PBS (168 μl), and centrifuged at 22,000 × *g* for 30 min. The supernatants were incubated in the absence or presence of anMan-containing HS oligosaccharide and disaccharide preparations (Aβ42:HS, 1:1, 1:3, or 1:5, w/w). Aβ A11 immunoreactivity was analyzed by slot blotting to PVDF membranes incubated with A11 (1:1000) or 4G8 (1:1000) antibodies

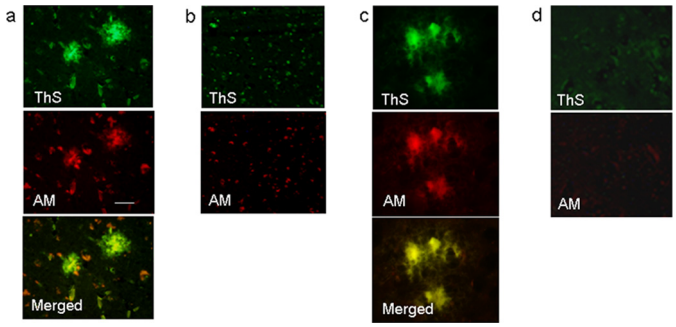

FIGURE 1. **Detection of anMan-containing products in amyloid plaques.** Immunofluorescence microscopy images of AD (*a*) and normal (*b*) human brain slices and Tg2576 (*c*) and wild-type (*d*) mouse brain slices stained for amyloid plaques using thioflavin S (*ThS*) and for anMan-containing HS degradation products using a specific mAb (*AM*) are shown. *Scale bar*, 50 μm.

followed by visualization using horseradish peroxidase-conjugated anti-rabbit IgG for A11 (1:500) and goat anti-mouse IgG for 4G8 (1:500). The oligomer state was monitored by SDS-PAGE on 4–12% Bis-Tris minigels in MES running buffer followed by silver staining (54).

Statistics—One-way analysis of variance was used to determine significance.

RESULTS

Detection of anMan-immunoreactive Products in Plaques from AD and Tg2576 Brains—Human brain sections were stained with thioflavin S and a mAb recognizing the anMan-containing epitope followed by immunofluorescence microscopy. The anti-anMan mAb was raised against deaminatively degraded heparin and has been described and characterized by Pejler *et al.* (80) (supplemental Fig. S1e). Amyloid plaques in AD brain slices that were stained with thioflavin S (Fig. 1*a*, *ThS*, *green*) also were stained for anMan-containing products (Fig. 1*a*, *AM*, *red*). The merged image indicated partial colocalization that was most intense in the center of the plaques (Fig. 1*a*, *Merged*, *yellow*). In age-matched normal human brain, there were small, scattered deposits of thioflavin S- and anMan-positive material (Fig. 1*b*).

Tg2576 mice are transgenic for the APP695 gene encoding the Swedish mutation K670N/M671L and are one of the most widely used animal models of AD (55, 56). The mice have plaques and cognitive deficits but no cell loss and no neurofibrillary tangles (44). Brain slices from Tg2576 mice were stained with thioflavin S and the anti-anMan antibody. There was colocalization between thioflavin S- and anMan-positive material with the greatest intensity in the center of the plaques (Fig. 1*c*, *Merged*, *yellow*). In wild-type mouse brain, there were small, diffuse, and scattered deposits of thioflavin S- and anMan-positive material (Fig. 1*d*).

Detection of Aβ, APP/APP-CTF, Aβ Oligomers, and anMan in Fibroblast Cultures by Immunofluorescence Microscopy— To examine whether there was intracellular colocalization between anMan-containing HS degradation products and APP degradation products, we performed cell culture studies using fibroblasts from wild-type and Tg2576 mice. The human APP transgene is expressed in Tg2576 fibroblasts as demonstrated by SDS-PAGE and Western blotting using mAb WO2, which is specific for the human Aβ sequence (supplemental Fig. S2).

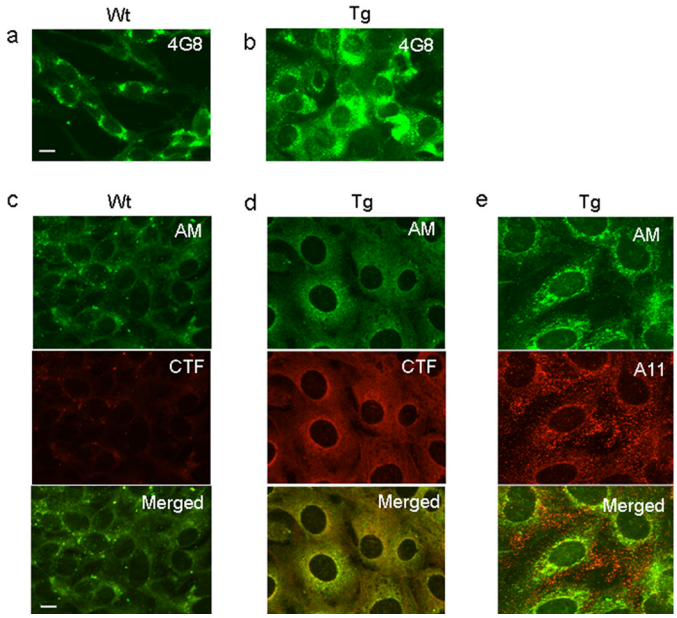

FIGURE 2. **Detection of Aβ, APP/APP-CTF, A11, and anMan immunoreactivity in fibroblasts.** The immunofluorescence microscopy images were obtained after staining cultures of wild-type (*Wt*) and Tg2576 (*Tg*) fibroblasts with the Aβ-specific mAb (*4G8*; *green*) (*a* and *b*) or the anMan-specific mAb (*AM*; *green*) (*c–e*) and the polyclonal anti-CTF A8717 (*CTF*; *red*) (*c* and *d*) or the Aβ oligomer-specific antibody A11 (*red*) (*e*). *Scale bar*, 10 μm. These experiments were repeated twice.

To investigate APP and HS degradation products in wild-type and Tg2576 fibroblasts, we used antibodies recognizing the Aβ region (mAb 4G8) or the C terminus of APP (polyclonal antibody A8717) as well as the anMan-containing epitope (mAb AM). Staining for both Aβ- and anMan-containing material was more intense in fibroblasts from Tg2576 mice than in corresponding cells from wild-type mice (Fig. 2*a* and *b*, *Aβ*, *green*, and *c* and *d*, *AM*, *green*). Staining using anti-APP-CTF was also more intense in Tg2576 cells than in wild-type cells (Fig. 2, *c* and *d*, *CTF*, *red*). APP/APP-CTF immunoreactivity colocalized with the anMan staining at perinuclear sites (Fig. 2*d*, *Merged*, *yellow*), but there was also separate anMan staining (Fig. 2*d*, *Merged*, *green*).

Aβ peptides may be converted into potentially toxic forms that can be recognized by the A11 antibody (8). It is our understanding that this antibody recognizes oligomeric forms and not fibrils. To search for possible colocalization between such oligomers and anMan-containing products, Tg2576 fibroblasts were stained for anMan and A11 immunoreactivity. There was limited colocalization, and most of the cytoplasmic A11 staining was located close to the plasma membrane and also extracellularly, whereas anMan staining dominated in the perinuclear area (Fig. 2*e*, *Merged*). No staining was observed when the primary antibody was omitted (data not shown).

Detection of anMan-immunoreactive, HS-containing APP Degradation Products in Tg2576 Fibroblasts by SDS-PAGE and Gel Exclusion Chromatography—The colocalization of anMan and APP-CTF immunoreactivity suggested an association between anMan-containing HS degradation products and APP or APP degradation products in Tg2576 fibroblasts. To search for co-precipitation and co-migration on SDS-PAGE of anMan and Aβ immunoreactivity, RIPA extracts of confluent Tg2576 fibroblast cultures were immunoprecipitated with either the anti-Aβ (H-43) or the anti-APP C-terminal (A8717) polyclonal antibodies. The immunoprecipitates were Western blotted using either the anMan- or the Aβ-specific (4G8) mAb. The results showed that the anti-Aβ (H-43) immunoprecipitate contained one specific anMan-positive species with an apparent molecular mass of approximately 50–55 kDa (Fig. 3*a*, *lanes 1* and *2*). Western blotting a parallel lane with the Aβ-specific mAb 4G8 stained a band in the same position (Fig. 3*a*, *lane 3*). A number of minor, 4G8-positive, anMan-negative species, ranging from approximately 20 to 60 kDa, were also observed. Immunoprecipitation using the anti-APP C-terminal antibody (A8717) yielded primarily the 50–55-kDa anMan- and Aβ(4G8)-positive species (Fig. 3*a*, *lanes 4–6*). No bands were observed when the primary antibody was omitted (Fig. 3*a*, *lanes 1* and *4*).

If HS oligosaccharides were bound to APP degradation products the complex should be negatively charged. To test this, polyanionic compounds were recovered from RIPA extracts of Tg2576 cells by binding to DEAE-cellulose, then released by 1 M NaCl, dialyzed, and subjected to immunoprecipitation using the APP C-terminal antibody followed by SDS-PAGE and Western blotting using the anMan-specific mAb. Again, a 50–55-kDa anMan-positive component was obtained (Fig. 3*a*, *lane 7*). As there were no bands at 90 kDa or higher, it appears likely that the anMan-containing HS degradation products were associated with APP-CTF-β, generating a negatively supercharged complex.

To degrade the protein part of a putative, SDS-stable HS·APP-CTF-β complex, an anti-APP-CTF immunoisolate from Tg2576 fibroblasts was subjected to SDS-PAGE after treatment with proteinase K. This resulted in partial degradation and in the generation of a 30–35-kDa anMan- and Aβ (4G8)-positive component (Fig. 3*b*, *lanes 1* and *2*), suggesting that anMan-containing HS degradation products were associated with the Aβ region of APP-CTF-β.

Treatments with the HS and heparin lyases gave somewhat surprising results. There was no major change in size of the putative complex upon either HS or heparin lyase treatment (Fig. 3*b*, *lanes 3–6*). However, the intensity of the 4G8 staining was markedly increased after treatment with heparin lyase (Fig. 3, *cf. b*, *lane 6* and *a*, *lane 6*). These results suggest that anMan-containing HS oligosaccharides associated with APP-CTF-β were small, were sensitive to heparin lyase, and interacted with the 4G8 epitope. Control experiments showed that the HS lyase preparation was active (57).

To generate radiolabeled HS·Aβ complexes, Tg2576 fibroblasts were incubated with $^{35}SO_4$, and polyanionic products were isolated from the cell lysate by passage over DEAE-cellulose. Recovered products were displaced with 4 M guanidinium chloride and chromatographed on a Superose 6 column in the same solvent. In addition to a major proteoglycan pool (Fig. 3*c*, *fractions 25–40*), a smaller, more retarded peak was observed (Fig. 3*c*, *fractions 41–49*, see *bar*). Analysis of this fraction by SDS-PAGE yielded a 4G8-positive band with an apparent molecular mass of 70–75 kDa (Fig. 3*c*, *inset*). Analysis by gel exclusion chromatography on a Superdex peptide column before and after treatment with HNO_2 at pH 1.5 demonstrated

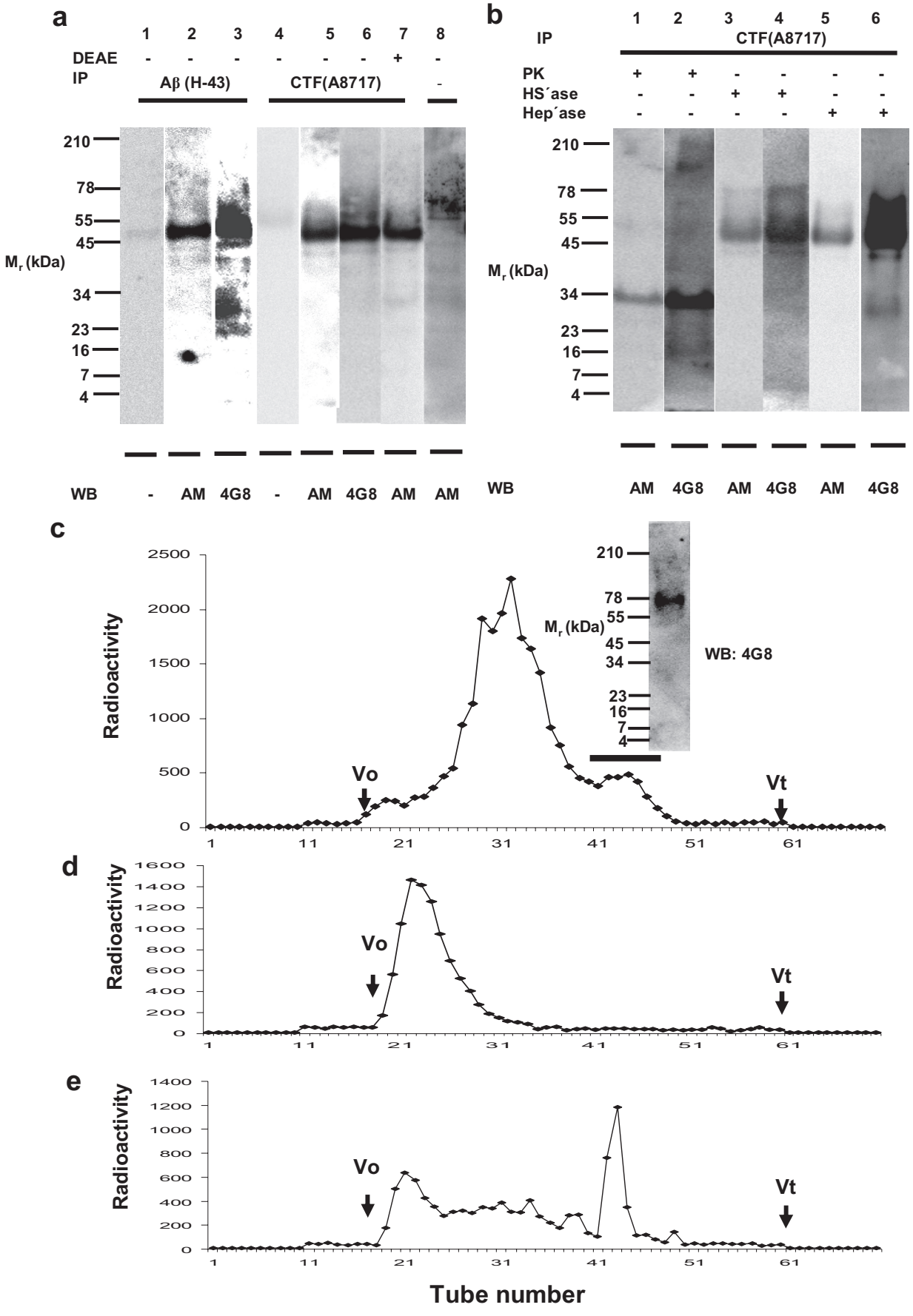
a
1 2 3 4 5 6 7 8
DEAE - - - - - - + -
IP Aβ (H-43) CTF(A8717) -
210
78
55
45
Mr (kDa)
34
23
16
7
4
WB - AM 4G8 - AM 4G8 AM AM
b
IP 1 2 3 4 5 6
CTF(A8717)
PK + + - - - -
HS´ase - - + + - -
Hep´ase - - - - + +
210
78
55
45
Mr (kDa)
34
23
16
7
4
WB AM 4G8 AM 4G8 AM 4G8
c
Radioactivity
2500
2000
1500
1000
500
0
Vo
Vt
210
78
55
45
34
23
16
7
4
Mr (kDa)
WB: 4G8
1 11 21 31 41 51 61
d
Radioactivity
1600
1400
1200
1000
800
600
400
200
0
Vo
Vt
1 11 21 31 41 51 61
e
Radioactivity
1400
1200
1000
800
600
400
200
0
Vo
Vt
1 11 21 31 41 51 61
Tube number

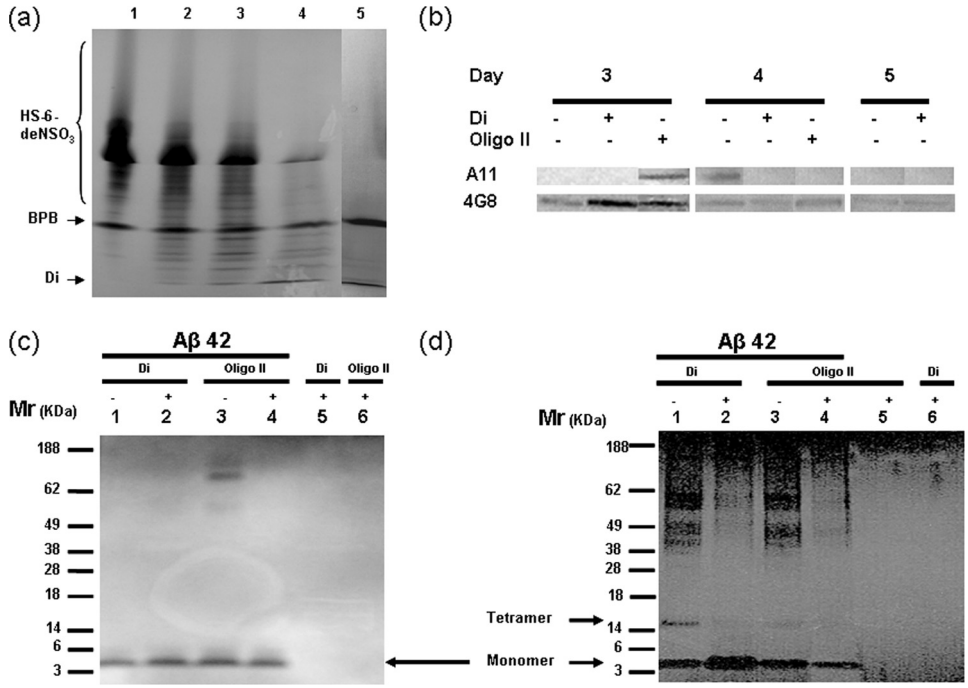

FIGURE 4. **Modulation of Aβ42 A11 immunoreactivity and oligomerization by anMan-containing HS oligosaccharides and disaccharides.** *a*, oligosaccharide PAGE of anMan-containing HS degradation products obtained by partial or complete deaminative cleavage at pH 3.9 of *N*-desulfated HS6. *Lane 1*, untreated HS; *lanes 2–4*, HS treated with HNO_2 reagent that was diluted 1:50 (*lane 2*), 1:25 (*lane 3*), or 1:10 (*lane 4*); *lane 5*, HS treated with undiluted reagent. Staining was performed with Alcian Blue. *HS-6-deNSO*$_3$, migration position of the charge and size polydisperse untreated HS; *BPB*, bromphenol blue; *Di*, disaccharide. *b*, slot blot of Aβ42 after incubation in the absence or presence of OligoII or disaccharides (*Di*) as indicated (Aβ:HS = 1:5, w/w). Aβ was detected using either the A11 antibody or mAb 4G8. *c* and *d*, SDS-PAGE of Aβ42 alone or exposed to OligoII or disaccharides (*Di*) as indicated (Aβ:HS = 1:5, w/w). In *c*, the samples were analyzed directly after mixing (Day 0), and in *d*, the samples were analyzed on Day 5.

the presence of HS (Fig. 3, *d* and *e*). The peak of free sulfate (Fig. 3*e*, *fractions 42–44*) should be generated from cleavage at *N*-sulfated glucosamine residues. The presence of oligosaccharides ranging in size from di- to decasaccharides indicated that also extended sequences containing *N*-acetylated glucosamine were present in this HS. The peak eluting closely after the void volume may represent HS stubs still attached to Aβ. As the radioactive HS·Aβ complexes were larger (70–75 kDa) than the resident material (50–55 kDa), the former may either contain longer HS oligosaccharides and/or represent higher Aβ oligomers.

Modulation of A11 Immunoreactivity and Oligomerization of Aβ42 Peptide by anMan-containing HS Oligo- and Disaccharides—The anMan-containing HS degradation products may largely interact reversibly with the Aβ domain in CTF-β or with Aβ peptides undergoing oligomerization. HS and HS degradation products interact, mostly nonspecifically, with basic sequences in proteins. The sequence HHQK in Aβ may thus constitute an HS-attracting site. To test possible conformational effects of anMan-containing HS degradation products on Aβ, we adopted a procedure whereby the conversion of monomeric Aβ42 to A11-positive oligomers can be monitored *in vitro* (53).

anMan-containing HS oligo- and disaccharide preparations were generated by partial or complete deaminative cleavage at pH 3.9 of *N*-desulfated HS6, a preparation where ~70% of the hexosamines should be *N*-unsubstituted and thus sensitive to cleavage by HNO_2. Degradation was monitored by PAGE, and the results are shown in Fig. 4*a*. Undegraded *N*-desulfated HS6, which is both charge and size polydisperse, migrated broadly but more slowly than the bromphenol blue marker (Fig. 4*a*, *lane 1*). Degradations with reagent that was diluted generated mainly oligosaccharide products (migrating faster than bromphenol blue; see Fig. 4*a*, *lanes 2–4*). The predominant product generated by undiluted reagent migrated as a disaccharide (Fig. 4*a*, *lane 5*). The preparations used in the experiments were

FIGURE 3. **Detection of anMan-immunoreactive, HS-containing APP degradation products in Tg2576 fibroblasts by SDS-PAGE and gel exclusion chromatography.** RIPA extracts (1 ml) of confluent fibroblast cultures containing 1 mg/ml protein were subjected to immunoisolation (*IP*) using anti-Aβ (H-43; 1:250) or anti-C-terminal APP (A8717; 1:500) followed by SDS-PAGE and transfer to PVDF membranes (*a*). Western blotting (*WB*) was performed with either the anMan-specific mAb AM (1:50) or the Aβ-specific mAb 4G8 (1:500). In the controls, precipitating or primary antibodies were omitted (−). In one case, the RIPA extract was passed through DEAE-cellulose (0.2 ml) to recover polyanionic compounds that were subsequently subjected to immunoisolation, SDS-PAGE, and Western blotting (*DEAE+*; *lane 7*). In *b*, anti-C-terminal APP immunoisolates (*IP*) recovered by binding to protein A were treated (+) with proteinase K (*PK*), HS lyase (*HS'ase*), or heparin lyase (*Hep'ase*) before electrophoresis. After treatment of the protein A-bound immunoisolates, salt was removed by dialysis against water, Novex Tricine-SDS sample buffer (from Invitrogen) was added, the sample was boiled, protein A was removed by centrifugation, and the supernatant was electrophoresed. Western blotting was performed as in *a*. In *c*, [^{35}S]sulfate-labeled, polyanionic products obtained from RIPA extracts of Tg2576 fibroblasts (6×10^6 cells) were recovered on DEAE-cellulose, displaced with 4 M guanidinium chloride, and chromatographed on Superose 6 in the same solvent. Aliquots of the fractions were analyzed for radioactivity by β-scintillation. Fractions 41–49 were pooled (see *bar* in *c*), and half of this material was precipitated with ethanol, dissolved in SDS, and subjected to SDS-PAGE followed by transfer to membranes that were probed with mAb 4G8 (*inset* in *c*). In *d* and *e*, equal amounts of the other half of the same pool (*41–49* in *c*) were chromatographed on Superdex peptide before (*d*) and after (*e*) treatment with HNO_2 at pH 1.5. Total radioactivity in each tube was recorded. V_0, void volume; V_t, total volume.

HS oligosaccharides (OligoII) (Fig. 4*a*, *lane 3*) and disaccharides (*lane 5*).

Unagitated, monomeric Aβ42 is spontaneously and transiently converted to an A11-positive conformation that oligomerizes (53). HS oligo- and disaccharides were added in an ~30-fold molar excess to Aβ42 monomer (assuming a disaccharide molecular weight of 600). This should correspond to an ~6-fold molar excess relative to the number of amino groups in Aβ (N terminus, Gln, Lys, Asn, and Lys). A11 immunoreactivity usually appeared at Day 4 (sometimes at Days 3 and 4) in the absence of HS oligo- or disaccharides (Fig. 4*b*). In the presence of the HS disaccharide preparation, no A11 immunoreactivity was observed. In the presence of partial HS degradation products (OligoII preparation), A11 immunoreactivity appeared at Day 3 instead of Day 4 (Fig. 4*b*). A11 immunoreactivity appeared somewhat later in our experiments than in those of Ladiwala *et al.* (53). 4G8 staining was enhanced by the disaccharide preparation at Day 3. No staining was observed when the primary antibody was omitted (data not shown).

The starting Aβ42 preparation (Day 0) was purely monomeric as judged by SDS-PAGE (Fig. 4*c*, *lane 1*). The presence of the anMan-containing HS disaccharide preparation did not alter the migration of Aβ42 (Fig. 4*c*, *lane 2*). In one case, when large aggregates had not been completely removed (Fig. 4*c*, *lane 3*), these were disrupted in the presence of the OligoII preparation (Fig. 4*c*, *lane 4*). However, the migration of monomeric Aβ42 was not altered in the presence of OligoII. It should be noted that HS oligo- and disaccharides were not detected by this staining technique (Fig. 4*c*, *lanes 5* and *6*).

The oligomer state of Aβ42 after a 5-day incubation with or without anMan-containing HS oligo- or disaccharides (6-fold molar excess relative to the number of amino groups in Aβ) was also assayed by SDS-PAGE (Fig. 4*d*). Samples not exposed to HS degradation products contained oligomers with a molecular mass greater than 40 kDa as well as tetramer and monomer (Fig. 4*d*, *lanes 1* and *3*). Incubation with the HS disaccharide preparation greatly inhibited formation of higher oligomers and tetramers (Fig. 4*d*, *lane 2*). Also, the OligoII preparation inhibited formation of higher oligomers (Fig. 4*d*, *lane 4*). As there was no increase in Aβ monomer in the latter case (Fig. 4*d*, *cf. lanes 2* and *4*), the longer HS oligosaccharides may have induced formation of insoluble Aβ aggregates. A 2-fold molar excess of HS disaccharide relative to amino groups did not inhibit Aβ42 oligomerization. However, a 2-fold molar excess of the OligoII preparation partially inhibited oligomerization (results not shown). In summary, these results indicate that an excess of small anMan-containing HS oligosaccharides, probably disaccharides, can modulate A11 immunoreactivity and inhibit the formation of higher oligomers without forming SDS-stable conjugates with Aβ. These results may thus explain why anMan and A11 immunoreactivity did not colocalize in Tg2576 fibroblasts (Fig. 2*e*).

Effect of Silencing Gpc-1 Expression or Treatment with U18666A on Aβ, anMan, and A11 Immunoreactivity in Tg2576 Fibroblasts—Because there are colocalization and a possible functional interplay between Gpc-1 and APP/Aβ, we examined the effect of Gpc-1 silencing on Aβ immunoreactivity in Tg2576 fibroblasts using the mAb 4G8. When Gpc-1 expression was suppressed almost 5-fold (Fig. 5*a*), there was more than a 2-fold increase in Aβ (4G8) immunoreactivity (Fig. 5*b*) as measured by flow cytometry, suggesting that Gpc-1 is involved in APP/Aβ processing.

NO-dependent degradation of Gpc-1 HS results in formation of anMan-containing HS degradation products that may modulate A11 immunoreactivity. These products accumulate in Rab7-positive endosomes (40, 41) and were also detected in Tg2576 fibroblasts (supplemental Fig. S3a). However, a portion of the anMan staining colocalized with LysoTracker Red in large vesicular structures (supplemental Fig. S3b).

Accumulation of anMan-containing HS degradation products in Rab7-positive endosomes diminishes when intra/interendosomal transport is blocked as in Niemann-Pick C1 fibroblasts or in normal fibroblasts exposed to the synthetic, cationic steroid U18666A, which mimics the disease (40, 41). Under both of these conditions, APP processing is also disturbed, and accumulation of Aβ and APP-CTF in endosomes has been observed (58–60). Accordingly, when Tg2576 fibroblasts were treated with U18666A, there was a 3–4-fold increase in Aβ (4G8) reactivity as measured by flow cytometry (Fig. 5*c*) and as recorded by immunofluorescence microscopy (Fig. 5, *d* and *e*, *green*). Moreover, U18666A-treated Tg2576 fibroblasts showed increased staining with the Aβ oligomer-selective antibody A11 (Fig. 5, *d* and *e*, *red*). Most of the A11 immunoreactivity colocalized with Aβ in U18666A-treated cells (Fig. 5*e*, *Merged*, *yellow*). However, anMan staining was only marginally suppressed by U18666A in Tg2576 fibroblasts (Fig. 5, *f* and *g*), whereas there is significant suppression in other cell types (40, 41).

To examine the effect of U18666A on the formation of the 50–55-kDa anMan- and Aβ-positive species, we performed SDS-PAGE. The anMan immunoreactivity was essentially unaffected (Fig. 5*h*, *lanes 3* and *4*), whereas the 4G8 immunoreactivity increased (Fig. 5*h*, *lanes 5* and *6*). This could reflect a change in Aβ conformation/epitope availability and/or accumulation of 50–55-kDa HS-CTF-β conjugates with a decreased HS-to-Aβ ratio. In the latter case, a reduction in size would be expected unless the 50–55-kDa component is oligomeric and the HS adduct consists of short oligosaccharides.

Effect of Ascorbate on Aβ and A11 Immunoreactivity in Untreated or U18666A-treated Tg2576 Fibroblasts—We have previously shown, using both purified Gpc-1 and cell cultures, that NO-catalyzed autoprocessing of Gpc-1 resulting in the release of anMan-containing HS oligosaccharides can be stimulated by treatment with ascorbate. NO released by ascorbate from Gpc-1-SNO initiates degradation of Gpc-1 HS (32–34, 36, 40, 41). To examine whether increased formation of anMan-positive HS degradation products affects Aβ A11 immunoreactivity, we used flow cytometry and immunofluorescence microscopy.

Ascorbate treatment of Tg2576 fibroblasts had no detectable effect on Aβ (4G8) staining intensity (Fig. 6, *a* and *b*, *green*), but it reduced A11 staining (Fig. 6, *a* and *b*, *red*) by more than 3-fold as measured by flow cytometry (Fig. 6, *a* and *b*, *middle panels*, *inset*). We also tested the effect of ascorbate on Tg2576 fibroblasts that had been pre-exposed to U18666A. The U18666A-treated cells continued to accumulate A11 immunoreactivity even during a 4 h-chase in fresh medium (Fig. 6*c*, *red*). However, when the chase

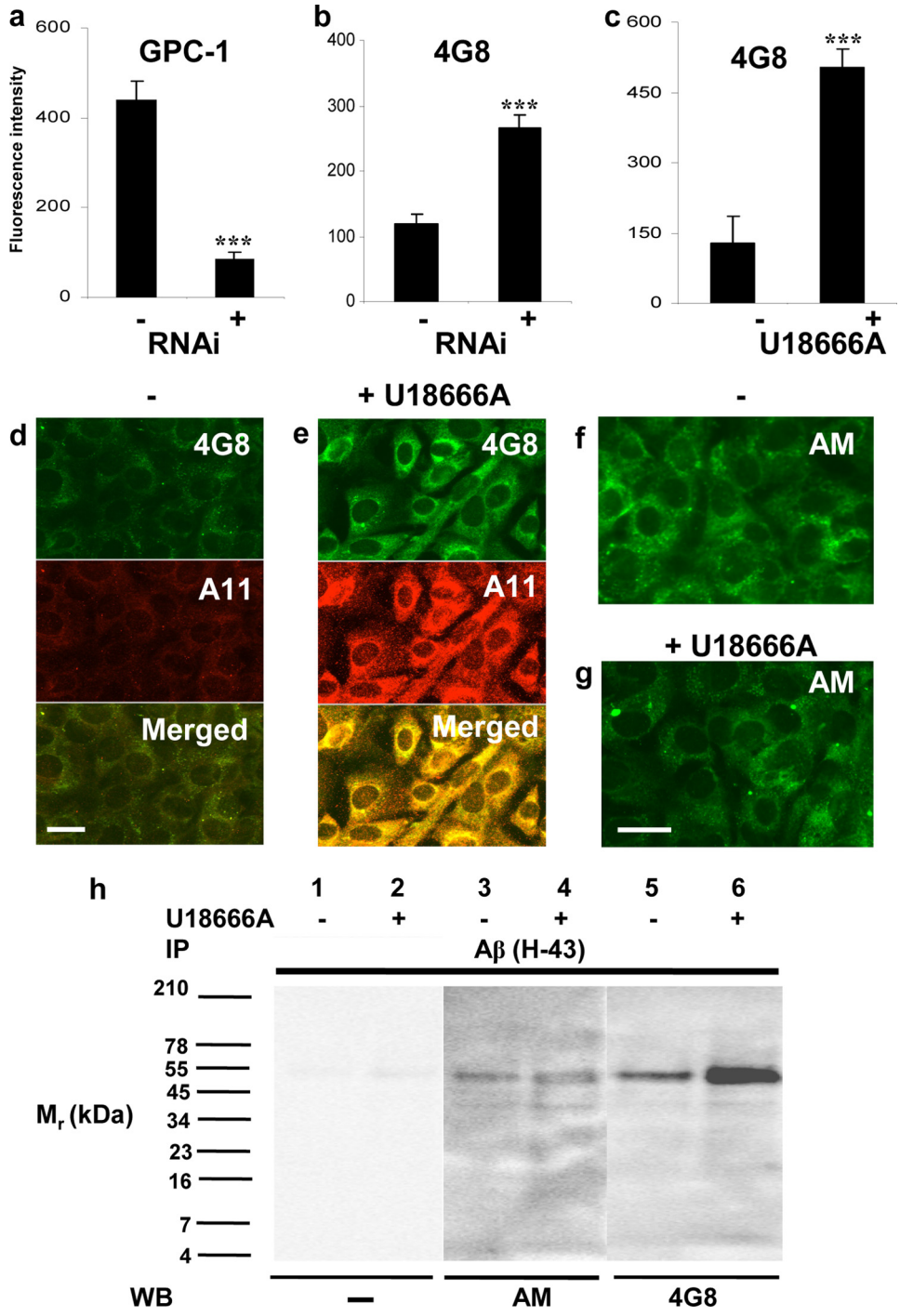

FIGURE 5. **Effect of silencing Gpc-1 expression or treatment with U18666A on Aβ, A11, and anMan immunoreactivity in Tg2576 fibroblasts.** The flow cytometry measurements (*a–c*) were obtained after staining mock- (−) or Gpc-1 RNAi-transfected (+) Tg2576 fibroblasts (*a* and *b*) for Gpc-1 using a polyclonal antibody (*a*) or Aβ using mAb 4G8 (*b*) and after staining untreated (−) or U18666A-treated (+) cells for Aβ using mAb 4G8 (*c*). The *error bars* indicate S.E.; ***, $p < 0.001$. The results of RNAi transfection were scored after 48 h of cell growth. The immunofluorescence microscopy images (*d–g*) were obtained after staining cultures of untreated (−) or U18666A-treated (+) Tg2576 fibroblasts for Aβ using mAb 4G8 (*green*) and the polyclonal antibody A11 (*red*), respectively (*d* and *e*), and for anMan-containing HS degradation products using mAb AM (*green*) (*f* and *g*). *Scale bar*, 20 μm. In *h*, SDS-PAGE was performed on Aβ (H-43) immunoisolates (*IP*) derived from untreated (−) or U18666A-treated (+) confluent Tg2576 fibroblast cultures followed by Western blotting (*WB*) with the anMan-specific mAb (*AM*) or the Aβ-specific mAb (*4G8*). Band intensities were estimated by densitometry. Treatment with 10 μg/ml U18666A was carried out for 16 h. These experiments were repeated twice.

medium included ascorbate, there was a reduction in A11 immunoreactivity (Fig. 6*d*, *red*) without much change in Aβ 4G8 immunoreactivity (Fig. 6, *c* and *d*, *green*). This indicates that an A11-positive conformation that was induced by treatment with U18666A could be reversed by ascorbate.

Effect of Gpc-1 Overexpression and/or Copper-NO Supplementation on Aβ A11 Immunoreactivity in Untreated or Ascorbate-treated Tg2576 Fibroblasts—A high intracellular level of *S*-nitrosylated Gpc-1 is a prerequisite for the formation of high quantities of anMan-containing HS oligosaccharides.

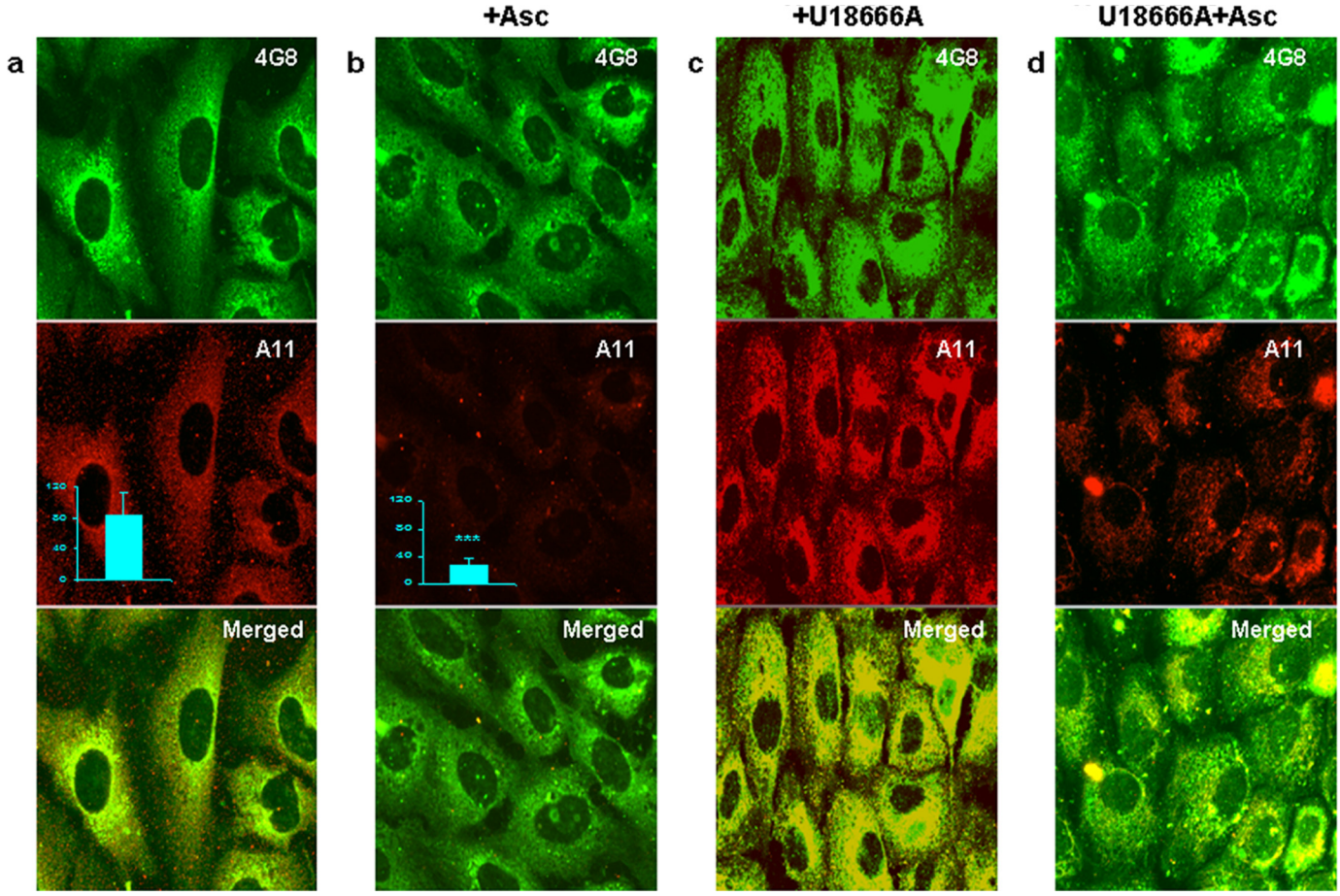

FIGURE 6. **Effect of ascorbate on Aβ and A11 immunoreactivity in untreated and U18666A-treated Tg2576 fibroblasts.** The immunofluorescence microscopy images were obtained after staining cultures of untreated (*a*), ascorbate-treated (+*Asc*) (*b*), U18666A- (*c*) or U18666A- and ascorbate (+*Asc*)-treated (*d*) Tg2576 fibroblasts for Aβ using mAb 4G8 (*green*) and for Aβ oligomers using the polyclonal antibody A11 (*red*), respectively. In *b*, treatment with 1 mM ascorbate was carried out for 4 h. In *c* and *d*, cells were first exposed to 10 μg/ml U18666A for 16 h and then chased in fresh medium with or without 1 mM ascorbate for an additional 4 h. *Scale bar*, 20 μm. The flow cytometry measurements (*inset* in *a* and *b*) were obtained after staining untreated or ascorbate-treated (+*Asc*) Tg2576 fibroblasts for Aβ oligomers using the polyclonal antibody A11. The *error bars* indicate S.E.; ***, $p < 0.001$.

To obtain Gpc-1 overexpression, the Tg2576 fibroblasts were transiently transfected with GFP-Gpc-1 (Fig. 7*a*, *green*). Colocalization between GFP-Gpc-1 and Aβ A11 immunoreactivity was restricted to perinuclear sites, whereas most of the GFP-Gpc-1 appeared throughout the cytoplasm (Fig. 7*a*, *Merged*).

Stimulation of *S*-nitrosylation with Cu(II) ions plus sodium nitroprusside (NO donor) had no dramatic effect on A11 staining either in GFP-Gpc-1-transfected (Fig. 7, *a* and *b*, *red*) or untransfected cells (Fig. 7, *e* and *f*). Subsequent treatment with ascorbate reduced A11 staining in transfected cells (Fig. 7*c*, *red*), whereas anMan staining increased (Fig. 7*d*, *AM*, *red*; *cf. inset* in *d*). In the untransfected Tg2576 fibroblasts, copper and NO supplementation followed by treatment with ascorbate almost completely eliminated A11 immunoreactivity (Fig. 7*g*), although the increase of anMan-containing products was less pronounced compared with transfected cells (Fig. 7, *h* and *inset* in *h*). When untransfected Tg2576 fibroblasts that had been exposed to copper, NO supplementation, and ascorbate were incubated in fresh medium for an additional 3h, A11 immunoreactivity reappeared (Fig. 7*g*, *inset*).

These results show that suppression of A11 immunoreactivity in Tg2576 fibroblasts correlates with increased generation of anMan-containing HS oligosaccharides and that the effect is greatly potentiated by preceding supplementation with copper and NO. Overexpression of Gpc-1 does not further potentiate suppression of A11 immunoreactivity probably because most of the GFP-Gpc-1 is present in compartments not containing Aβ. The results also show that sustained suppression of A11 immunoreactivity requires a constant supply of ascorbate.

Detection of anMan- and Aβ-immunoreactive Components and Suppression of A11 Immunoreactivity in Brains from 3xTg-AD Mice—3xTg-AD mice, which express mutant APP (APPswe), tau (P301L), and presenilin 1 (M146V), have a pathology that more closely resembles human AD. At 15–20 months of age, their brains contain high amounts of A11-immunoreactive material primarily located in extracellular sites in the hippocampus (18). We first examined whole brain extracts from 15-month-old mice for the presence of anMan- and Aβ-immunoreactive components. SDS-PAGE and Western blotting revealed the presence of the 50–55-kDa species but also some species of lower molecular size, in particular a 30-kDa component (Fig. 8*a*).

We then analyzed slices of hippocampus from these mice for both anMan and A11 immunoreactivity by immunofluores-

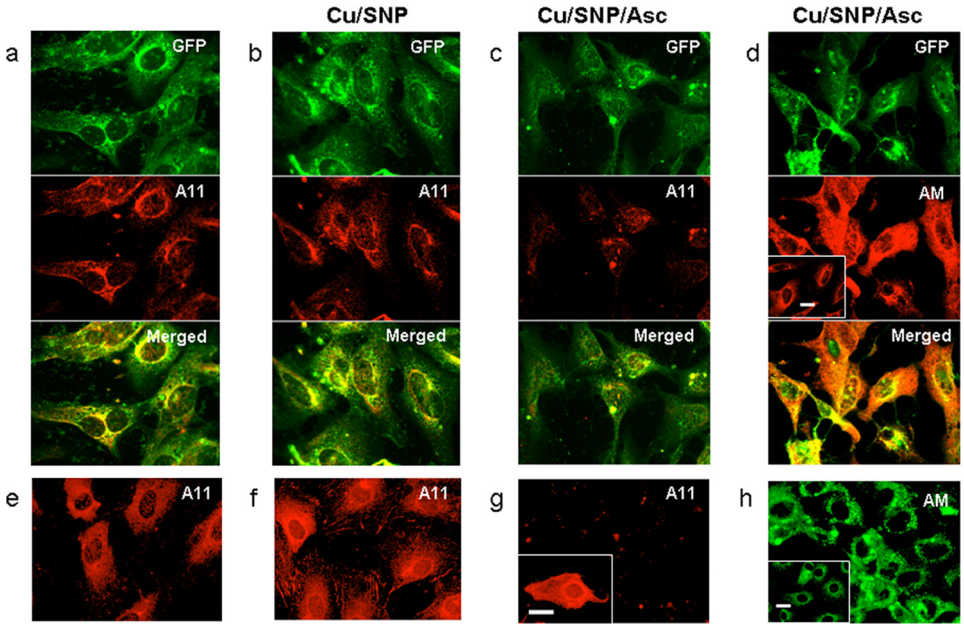

FIGURE 7. **Effect of ectopic expression of GFP-Gpc-1 and/or copper-NO supplementation on Aβ A11 immunoreactivity in untreated or ascorbate-treated Tg2576 fibroblasts.** The immunofluorescence microscopy images show GFP-Gpc-1-transfected (*a–d*; *green*) or untransfected Tg2576 fibroblasts (*e–h*) that were untreated (*a* and *e*), exposed to medium containing 0.1 mM $CuCl_2$ and 1 mM sodium nitroprusside (*Cu/SNP*) for 1 h (*b* and *f*), or exposed to medium containing 0.1 mM $CuCl_2$ and 1 mM sodium nitroprusside for 1 h and then with fresh medium containing 1 mM ascorbate (*Cu/SNP/Asc*) for 3 h (*c*, *d*, *g*, and *h*) followed by staining for Aβ oligomers using the polyclonal antibody A11 (*red*) (*a–c* and *e–g*) or anMan-containing products using mAb AM (*d* (*red*) and *h* (*green*)). The *inset* in *g* shows A11 staining of untransfected cells that were incubated in fresh medium for 3 h after sequential exposure to $CuCl_2$, sodium nitroprusside, and ascorbate. The *insets* in *d* and *h* show staining of untreated GFP-Gpc-1-transfected (*d*) or untransfected cells (*h*) for anMan-containing products using mAb AM. *Scale bars*, 20 μm.

cence microscopy. Strong staining with both antibodies was seen throughout the tissue (Fig. 8*b*, *green* and *red*). Incubation in medium containing Cu(II) ions and NO donor did not much affect the staining intensities (Fig. 8*c*). Most strikingly, subsequent exposure to ascorbate almost completely eliminated A11 immunoreactivity (Fig. 8*d*, *red*). As staining for anMan was strong already in untreated slices, additional formation of anMan-containing HS degradation products was only marginal (Fig. 8, *b–d*, *green*).

DISCUSSION

APP is a precursor to the amyloidogenic Aβ peptides in AD, but the normal function of APP and its degradation products remains poorly understood. The N-terminal ectodomain is growth factor-like and has a neurotrophic role, whereas the cytoplasmic C terminus participates in cell adhesion and gene regulation (for recent reviews, see Refs. 61 and 62). The Aβ peptides can assume a number of oligomeric conformations, some of which may be pore-forming (9, 63, 64). Whether this property is only a pathological feature remains unknown (65).

Aβ oligomers (size range, 40–60 kDa) may be responsible for the neurotoxicity in AD (for reviews, see Refs. 6 and 62). Moreover, Aβ can efficiently generate reactive oxygen species in the presence of transition metals, such as copper, and form *e.g.* carbonyl groups in amino acid side chains or stable dityrosine-cross-linked dimers (66). APP itself can also form dimers and oligomers, which are the likely physiological substrates for β-secretase (67–69). If the generated APP-CTF-β fragments remain oligomeric, this may facilitate Aβ peptide oligomerization upon subsequent cleavage by γ-secretase (Fig. 9*a*).

Tg2576 fibroblasts express a mutant APP that is especially sensitive to β-secretase cleavage, resulting in increased production of APP-CTF-β compared with wild-type cells. Here, we show that this is accompanied by increased formation of anMan-containing HS degradation products that colocalize with APP-CTF-β. We also show that anMan-containing HS oligosaccharides and especially disaccharides modulate/suppress Aβ A11 immunoreactivity and Aβ oligomerization *in vitro*. As the NO-sensitive $GlcNH_3^+$ moieties are often clustered in Gpc-1 HS (70), anMan-containing di- and tetrasaccharides should be prominent products when NO-catalyzed HS degradation is stimulated by ascorbate *in vivo*. Moreover, as Gpc-1 colocalizes with APP, a high local concentration of anMan-containing HS oligosaccharides may be generated.

The reaction Aβ + HS-Di ↔ Aβ·HS-Di (where Di represents disaccharide), which probably involves aldimine formation, should have an equilibrium far to the left. Therefore, a large excess of HS disaccharide may be required to generate sufficient complex formation. In cultured Tg2576 fibroblasts, some of the HS·CTF-β complexes appear to be converted to 50–55-kDa, negatively charged, SDS-stable, oligomeric HS-CTF-β conjugates. anMan-Aβ aldimines may be stabilized by reduction in late endosomes. Alternatively, prolonged exposure of Aβ to an excess of anMan-containing saccharides can result in the rearrangement of the aldimines, generating a form of protein glycation.

A portion of newly synthesized HS in Tg2576 cells co-chromatographed with a 70–75-kDa Aβ-immunoreactive species, suggesting that resident 50–55-kDa HS-CTF-β conjugates were derived from a larger precursor possibly with longer

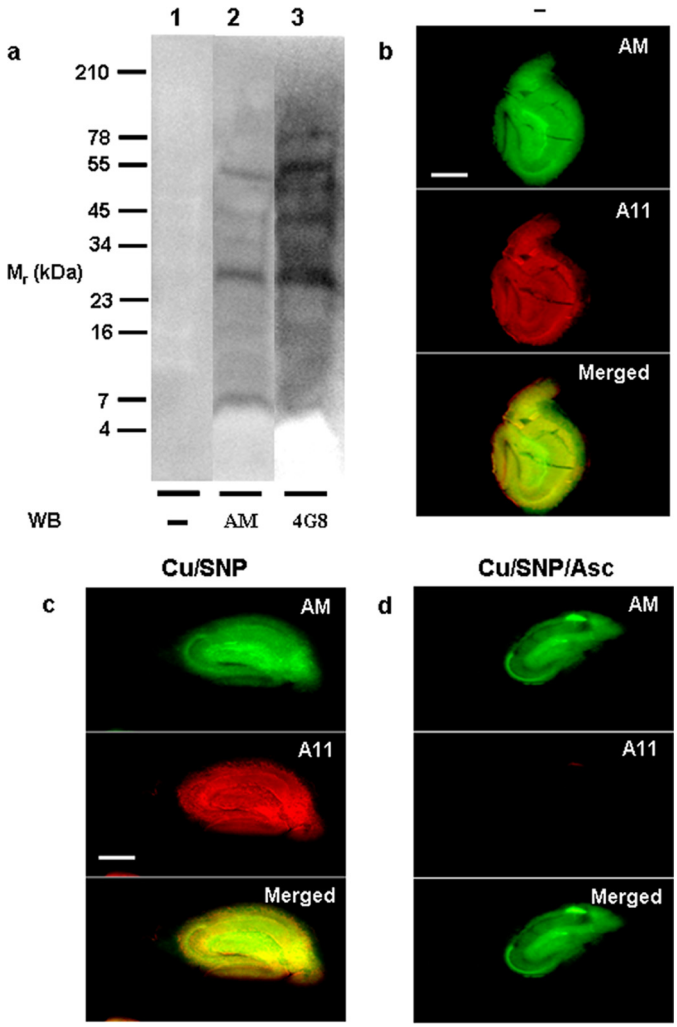

FIGURE 8. **Detection of anMan- and Aβ 4G8-immunoreactive components in extracts of whole brain and suppression of A11 immunoreactivity in slices of hippocampus from 15-month-old 3xTg-AD mice.** *a*, RIPA extracts of brain were subjected to SDS-PAGE followed by Western blotting (*WB*) using the mAbs AM and 4G8 as shown in Fig. 3. The immunofluorescence microscopy images were obtained after incubating slices with culture medium (*b*), culture medium containing 0.1 mM $CuCl_2$ and 1 mM sodium nitroprusside (*Cu/SNP*) for 1 h (*c*), or culture medium containing 0.1 mM $CuCl_2$ and 1 mM sodium nitroprusside for 1 h and then with fresh medium containing 1 mM ascorbate (*Cu/SNP/Asc*) for 3 h (*d*) followed by staining for anMan-containing HS degradation products using mAb AM (*green*) and for Aβ oligomers using the polyclonal antibody A11 (*red*). *Scale bar*, 500 μm.

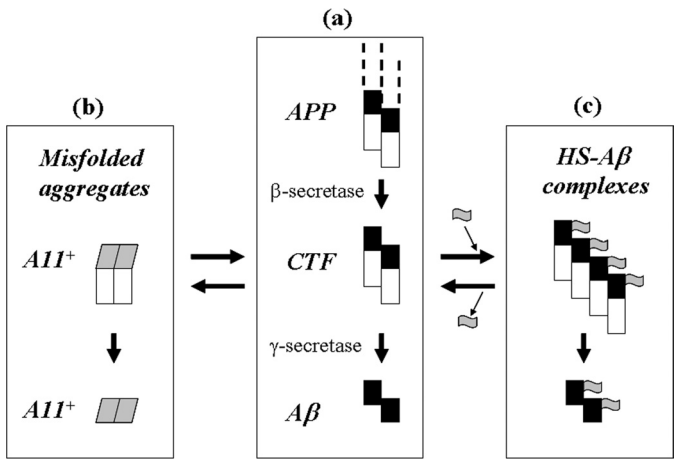

FIGURE 9. **Postulated role for HS in regulation of Aβ conformation.** *a*, APP (depicted as a dimer with N-terminal part not shown, Aβ domain in *black*, and C-terminal domain in *white*) is processed by β-secretase to CTF and subsequently by γ-secretase to Aβ. *b*, CTFs and Aβ may assume an A11-positive Aβ conformation (*gray*) and aggregate to higher oligomers (not shown). *c*, CTFs that reversibly interact with HS oligosaccharides (*gray flags*) may retain a nontoxic Aβ conformation. Secreted Aβ derived from such CTFs may sometimes contain covalently bound HS, which may ultimately appear in plaques.

N-acetylated glucosamine-containing HS oligosaccharide adducts. Endoheparanase and exoglycosidases may then degrade these oligosaccharides to the shorter, possibly highly sulfated stubs that were resistant to degradation by the bacterial HS lyase.

An APP-CTF-β tetramer should have an molecular mass of approximately 40 kDa. If the 50–55-kDa component is a tetrameric HS-APP-CTF-β conjugate, the HS adduct should amount to approximately 2.5–3.8 kDa in each Aβ domain. As there are at least three amino groups in Aβ that could be used as binding sites for anMan-containing HS oligosaccharides, each adduct may be very small (supplemental Fig. S1e).

Tg2576 fibroblasts displayed A11 immunoreactivity, indicating the presence of potentially toxic Aβ oligomers. However, the A11-positive material appeared to be mainly located separately from the anMan immunoreactivity. In general, accumulation of misfolded proteins is accompanied by increased formation of anMan-containing HS oligosaccharides as observed previously in tumor cells (43) and scrapie-infected neuronal cells (71) and now in hippocampal slices from 3xTg-AD mice (Fig. 8). In scrapie-infected neural cells, the anMan-positive HS degradation products co-immunoprecipitated and co-migrated with the scrapie prions, suggesting that anMan-containing HS oligosaccharides were covalently bound.

U18666A treatment markedly increased A11 immunoreactivity in Tg2576 fibroblasts. U18666A impedes transport from early to late endosomes and suppresses formation of anMan-containing HS oligosaccharides from Gpc-1 in normal fibroblasts and in T24 carcinoma and N2a neuroblastoma cell lines (40, 41). However, in Tg2576 fibroblasts, suppression of HS degradation was less pronounced. It is possible that Gpc-1 autoprocessing is maximally stimulated in Tg2576 cells and that HS-depleted HS-CTF-β conjugates accumulate in early endosomes of drug-treated cells. Excessive APP processing in combination with inadequate generation of HS degradation products may result in accumulation of oligomers selectively recognized by antibody A11 (Fig. 9, *a* and *b*).

Ascorbate releases NO from Gpc-1-SNO, which results in deaminative degradation of HS, generating more anMan-containing HS oligosaccharides. As shown here, treatment with ascorbate suppresses A11 immunoreactivity. This was demonstrated *in vitro* with untreated as well as U18666A-treated Tg2576 fibroblasts, with GFP-Gpc-1-transfected fibroblasts, and by *ex vivo* incubation of slices of hippocampus from 3xTg-AD mice. The effect of ascorbate was greatly potentiated by supplementation with Cu(II) ion and NO donor. A11 immunoreactivity that was almost completely eliminated in Tg2576 fibroblasts reappeared when ascorbate was withdrawn. This indicates that the A11-positive conformation is reversible. There may also be a rapid turnover of A11-positive higher oligomers, and fewer A11-positive smaller oligomers should be

formed when the generation of anMan-containing HS degradation products is stimulated by ascorbate.

We speculate that reversible and temporary interaction of APP-CTF-β with anMan-containing HS oligosaccharides modulates the conformation of the Aβ portion of APP-CTF-β. This may serve to maintain the Aβ domain in a non-toxic conformation after cleavage by γ-secretase (Fig. 9*c*). HS·Aβ complexes (temporary or permanent) are negatively supercharged, which may also limit oligomer/aggregate formation and confer resistance to proteolytic degradation. In AD, there may be insufficient formation of HS oligosaccharides to meet the needs, resulting in secretion of partially conjugated Aβ oligomers as indicated by the presence of anMan-containing HS in AD plaques.

Other studies indirectly support a role for Gpc-1 in APP processing and Aβ clearance. It was recently reported that removal of NO synthase 2 in APP transgenic mice resulted in a greater spectrum of Aβ-like pathologies (72). As NO is required for *S*-nitrosylation of Gpc-1, NO-catalyzed deaminative cleavage of the HS chains in Gpc-1 and subsequent formation of HS oligosaccharides would be diminished. Moreover, formation of anMan-containing HS oligosaccharides is markedly reduced when pre-endosomal cholesterol traffic is slow or blocked as in Niemann-Pick type C disease (40, 41). Indeed, aberrant cholesterol transport is associated with accumulation of APP-CTF-β and Aβ peptides (73, 74). Modulation of APP processing can also be achieved upstream of APP-CTF-β formation. sorLA/LR11 (75) and ubiquilin 1 (76) are examples of proteins that can affect early steps in the trafficking of APP. Thus, Gpc-1 is yet another protein involved in regulating APP processing but that is downstream of β-cleavage.

Finally, it is remarkable that it takes three different mutations to generate AD-like pathology in mice, whereas humans without mutations in any of these genes can spontaneously develop AD. There are indeed many differences between mice and men, but one is that mice can synthesize ascorbate, whereas humans cannot. It is well documented that ascorbate is important for neuroprotection, and certain neurons may contain up to 10 mM ascorbate (for reviews, see Refs. 77 and 78). Moreover, administration of ascorbate reduces spatial learning deficits in APP/PSEN1 transgenic mice (79). The present study supports the possibility that intracellular copper dysregulation, failing NO production, and/or an inadequate supply of vitamin C could contribute to late onset AD in humans.

Acknowledgments—We thank Prof. Gunnar Pejler, Uppsala University, and Prof. Peter Påhlsson, Linköping University, for generous gifts of monoclonal antibodies. We also thank Dr. Håkan Toresson, Lund University, for help with transfer of 3xTg-AD mice and Sol Da Rocha Baez for excellent technical assistance.

REFERENCES

1. Tanzi, R. E., Gusella, J. F., Watkins, P. C., Bruns, G. A., St George-Hyslop, P., Van Keuren, M. L., Patterson, D., Pagan, S., Kurnit, D. M., and Neve, R. L. (1987) *Science* **235,** 880–884
2. Kang, J., Lemaire, H. G., Unterbeck, A., Salbaum, J. M., Masters, C. L., Grzeschik, K. H., Multhaup, G., Beyreuther, K., and Müller-Hill, B. (1987) *Nature* **325,** 733–736
3. Hesse, L., Beher, D., Masters, C. L., and Multhaup, G. (1994) *FEBS Lett.* **349,** 109–116
4. Small, D. H., Nurcombe, V., Reed, G., Clarris, H., Moir, R., Beyreuther, K., and Masters, C. L. (1994) *J. Neurosci.* **14,** 2117–2127
5. McLean, C. A., Cherny, R. A., Fraser, F. W., Fuller, S. J., Smith, M. J., Beyreuther, K., Bush, A. I., and Masters, C. L. (1999) *Ann. Neurol.* **46,** 860–866
6. Haass, C., and Selkoe, D. J. (2007) *Nat. Rev. Mol. Cell Biol.* **8,** 101–112
7. LaFerla, F. M., Green, K. N., and Oddo, S. (2007) *Nat. Rev. Neurosci.* **8,** 499–509
8. Glabe, C. G. (2008) *J. Biol. Chem.* **283,** 29639–29643
9. Roychaudhuri, R., Yang, M., Hoshi, M. M., and Teplow, D. B. (2009) *J. Biol. Chem.* **284,** 4749–4753
10. Lee, S. J., Liyanage, U., Bickel, P. E., Xia, W., Lansbury, P. T., Jr., and Kosik, K. S. (1998) *Nat. Med.* **4,** 730–734
11. Morishima-Kawashima, M., and Ihara, Y. (1998) *Biochemistry* **37,** 15247–15253
12. Parvathy, S., Hussain, I., Karran, E. H., Turner, A. J., and Hooper, N. M. (1999) *Biochemistry* **38,** 9728–9734
13. Ehehalt, R., Keller, P., Haass, C., Thiele, C., and Simons, K. (2003) *J. Cell Biol.* **160,** 113–123
14. Watanabe, N., Araki, W., Chui, D. H., Makifuchi, T., Ihara, Y., and Tabira, T. (2004) *FASEB J.* **18,** 1013–1015
15. Takahashi, R. H., Milner, T. A., Li, F., Nam, E. E., Edgar, M. A., Yamaguchi, H., Beal, M. F., Xu, H., Greengard, P., and Gouras, G. K. (2002) *Am. J. Pathol.* **161,** 1869–1879
16. Takahashi, R. H., Almeida, C. G., Kearney, P. F., Yu, F., Lin, M. T., Milner, T. A., and Gouras, G. K. (2004) *J. Neurosci.* **24,** 3592–3599
17. Oddo, S., Caccamo, A., Shepherd, J. D., Murphy, M. P., Golde, T. E., Kayed, R., Metherate, R., Mattson, M. P., Akbari, Y., and LaFerla, F. M. (2003) *Neuron* **39,** 409–421
18. Oddo, S., Caccamo, A., Tran, L., Lambert, M. P., Glabe, C. G., Klein, W. L., and LaFerla, F. M. (2006) *J. Biol. Chem.* **281,** 1599–1604
19. Rajendran, L., Honsho, M., Zahn, T. R., Keller, P., Geiger, K. D., Verkade, P., and Simons, K. (2006) *Proc. Natl. Acad. Sci. U.S.A.* **103,** 11172–11177
20. Vingtdeux, V., Hamdane, M., Loyens, A., Gelé, P., Drobeck, H., Bégard, S., Galas, M. C., Delacourte, A., Beauvillain, J. C., Buée, L., and Sergeant, N. (2007) *J. Biol. Chem.* **282,** 18197–18205
21. Sharples, R. A., Vella, L. J., Nisbet, R. M., Naylor, R., Perez, K., Barnham, K. J., Masters, C. L., and Hill, A. F. (2008) *FASEB J.* **22,** 1469–1478
22. Motamedi-Shad, N., Monsellier, E., Torrassa, S., Relini, A., and Chiti, F. (2009) *J. Biol. Chem.* **284,** 29921–29934
23. Li, J. P., Galvis, M. L., Gong, F., Zhang, X., Zcharia, E., Metzger, S., Vlodavsky, I., Kisilevsky, R., and Lindahl, U. (2005) *Proc. Natl. Acad. Sci. U.S.A.* **102,** 6473–6477
24. Snow, A. D., Mar, H., Nochlin, D., Kimata, K., Kato, M., Suzuki, S., Hassell, J., and Wight, T. N. (1988) *Am. J. Pathol.* **133,** 456–463
25. Snow, A. D., Mar, H., Nochlin, D., Sekiguchi, R. T., Kimata, K., Koike, Y., and Wight, T. N. (1990) *Am. J. Pathol.* **137,** 1253–1270
26. Snow, A. D., Sekiguchi, R. T., Nochlin, D., Kalaria, R. N., and Kimata, K. (1994) *Am. J. Pathol.* **144,** 337–347
27. van Horssen, J., Otte-Höller, I., David, G., Maat-Schieman, M. L., van den Heuvel, L. P., Wesseling, P., de Waal, R. M., and Verbeek, M. M. (2001) *Acta Neuropathol.* **102,** 604–614
28. Wilhelmus, M. M., de Waal, R. M., and Verbeek, M. M. (2007) *Mol. Neurobiol.* **35,** 203–216
29. O'Callaghan, P., Sandwall, E., Li, J. P., Yu, H., Ravid, R., Guan, Z. Z., van Kuppevelt, T. H., Nilsson, L. N., Ingelsson, M., Hyman, B. T., Kalimo, H., Lindahl, U., Lannfelt, L., and Zhang, X. (2008) *Brain Pathol.* **18,** 548–561
30. Williamson, T. G., Mok, S. S., Henry, A., Cappai, R., Lander, A. D., Nurcombe, V., Beyreuther, K., Masters, C. L., and Small, D. H. (1996) *J. Biol. Chem.* **271,** 31215–31221
31. Fransson, L. Å., Belting, M., Cheng, F., Jönsson, M., Mani, K., and Sandgren, S. (2004) *Cell. Mol. Life Sci.* **61,** 1016–1024
32. Cheng, F., Mani, K., van den Born, J., Ding, K., Belting, M., and Fransson, L. Å. (2002) *J. Biol. Chem.* **277,** 44431–44439
33. Ding, K., Mani, K., Cheng, F., Belting, M., and Fransson, L. Å. (2002) *J. Biol. Chem.* **277,** 33353–33360

34. Mani, K., Cheng, F., Havsmark, B., Jönsson, M., Belting, M., and Fransson, L. Å. (2003) *J. Biol. Chem.* **278,** 38956–38965
35. Svensson, G., and Mani, K. (2009) *Glycoconj. J.* **26,** 1247–1257
36. Mani, K., Cheng, F., Havsmark, B., David, S., and Fransson, L. Å. (2004) *J. Biol. Chem.* **279,** 12918–12923
37. Cheng, F., Lindqvist, J., Haigh, C. L., Brown, D. R., and Mani, K. (2006) *J. Neurochem.* **98,** 1445–1457
38. Cappai, R., Cheng, F., Ciccotosto, G. D., Needham, B. E., Masters, C. L., Multhaup, G., Fransson, L. Å., and Mani, K. (2005) *J. Biol. Chem.* **280,** 13913–13920
39. Fivaz, M., Vilbois, F., Thurnheer, S., Pasquali, C., Abrami, L., Bickel, P. E., Parton, R. G., and van der Goot, F. G. (2002) *EMBO J.* **21,** 3989–4000
40. Mani, K., Cheng, F., and Fransson, L. Å. (2006) *Glycobiology* **16,** 711–718
41. Mani, K., Cheng, F., and Fransson, L. Å. (2006) *Glycobiology* **16,** 1251–1261
42. Fransson, L. Å., and Mani, K. (2007) *Trends Mol. Med.* **13,** 143–149
43. Mani, K., Cheng, F., and Fransson, L. Å. (2007) *J. Biol. Chem.* **282,** 21934–21944
44. Hsiao, K., Chapman, P., Nilsen, S., Eckman, C., Harigaya, Y., Younkin, S., Yang, F., and Cole, G. (1996) *Science* **274,** 99–102
45. Fransson, L. Å., Sjöberg, I., and Havsmark, B. (1980) *Eur. J. Biochem.* **106,** 59–69
46. Inoue, Y., and Nagasawa, K. (1976) *Carbohydr. Res.* **46,** 87–95
47. Mani, K., Jönsson, M., Edgren, G., Belting, M., and Fransson, L. Å. (2000) *Glycobiology* **10,** 577–586
48. Fransson, L. Å., Havsmark, B., and Silverberg, I. (1990) *Biochem. J.* **269,** 381–388
49. Belting, M., Mani, K., Jönsson, M., Cheng, F., Sandgren, S., Jonsson, S., Ding, K., Delcros, J. G., and Fransson, L. Å. (2003) *J. Biol. Chem.* **278,** 47181–47189
50. Bussière, T., Bard, F., Barbour, R., Grajeda, H., Guido, T., Khan, K., Schenk, D., Games, D., Seubert, P., and Buttini, M. (2004) *Am. J. Pathol.* **165,** 987–995
51. Rytter, A., Cronberg, T., Asztély, F., Nemali, S., and Wieloch, T. (2003) *J. Cereb. Blood Flow Metab.* **23,** 23–33
52. Necula, M., Kayed, R., Milton, S., and Glabe, C. G. (2007) *J. Biol. Chem.* **282,** 10311–10324
53. Ladiwala, A. R., Lin, J. C., Bale, S. S., Marcelino-Cruz, A. M., Bhattacharya, M., Dordick, J. S., and Tessier, P. M. (2010) *J. Biol. Chem.* **285,** 24228–24237
54. Shevchenko, A., Wilm, M., Vorm, O., and Mann, M. (1996) *Anal. Chem.* **68,** 850–858
55. McGowan, E., Eriksen, J., and Hutton, M. (2006) *Trends Genet.* **22,** 281–289
56. Morrissette, D. A., Parachikova, A., Green, K. N., and LaFerla, F. M. (2009) *J. Biol. Chem.* **284,** 6033–6037
57. Svensson, G., Linse, S., and Mani, K. (2009) *Biochemistry* **48,** 9994–10004
58. Yamazaki, T., Chang, T. Y., Haass, C., and Ihara, Y. (2001) *J. Biol. Chem.* **276,** 4454–4460
59. Jin, L. W., Shie, F. S., Maezawa, I., Vincent, I., and Bird, T. (2004) *Am. J. Pathol.* **164,** 975–985
60. Davis, W., Jr. (2008) *Curr. Alzheimer Res.* **5,** 448–456
61. Thinakaran, G., and Koo, E. H. (2008) *J. Biol. Chem.* **283,** 29615–29619
62. Querfurth, H. W., and LaFerla, F. M. (2010) *N. Engl. J. Med.* **362,** 329–344
63. Yoshiike, Y., Kayed, R., Milton, S. C., Takashima, A., and Glabe, C. G. (2007) *Neuromolecular Med.* **9,** 270–275
64. Kayed, R., Pensalfini, A., Margol, L., Sokolov, Y., Sarsoza, F., Head, E., Hall, J., and Glabe, C. (2009) *J. Biol. Chem.* **284,** 4230–4237
65. Lashuel, H. A., Hartley, D., Petre, B. M., Walz, T., and Lansbury, P. T., Jr. (2002) *Nature* **418,** 291–293
66. Cappai, R., and Barnham, K. J. (2008) *Neurochem. Res.* **33,** 526–532
67. Multhaup, G. (2006) *Neurodegener. Dis.* **3,** 270–274
68. Kaden, D., Munter, L. M., Joshi, M., Treiber, C., Weise, C., Bethge, T., Voigt, P., Schaefer, M., Beyermann, M., Reif, B., and Multhaup, G. (2008) *J. Biol. Chem.* **283,** 7271–7279
69. Munter, L. M., Botev, A., Richter, L., Hildebrand, P. W., Althoff, V., Weise, C., Kaden, D., and Multhaup, G. (2010) *J. Biol. Chem.* **285,** 21636–21643
70. Ding, K., Jönsson, M., Mani, K., Sandgren, S., Belting, M., and Fransson, L. Å. (2001) *J. Biol. Chem.* **276,** 3885–3894
71. Löfgren, K., Cheng, F., Fransson, L. Å., Bedecs, K., and Mani, K. (2008) *Eur. J. Neurosci.* **28,** 964–972
72. Wilcock, D. M., Lewis, M. R., Van Nostrand, W. E., Davis, J., Previti, M. L., Gharkholonarehe, N., Vitek, M. P., and Colton, C. A. (2008) *J. Neurosci.* **28,** 1537–1545
73. Burns, M., Gaynor, K., Olm, V., Mercken, M., LaFrancois, J., Wang, L., Mathews, P. M., Noble, W., Matsuoka, Y., and Duff, K. (2003) *J. Neurosci.* **23,** 5645–5649
74. Nixon, R. A. (2007) *J. Cell Sci.* **120,** 4081–4091
75. Andersen, O. M., Schmidt, V., Spoelgen, R., Gliemann, J., Behlke, J., Galatis, D., McKinstry, W. J., Parker, M. W., Masters, C. L., Hyman, B. T., Cappai, R., and Willnow, T. E. (2006) *Biochemistry* **45,** 2618–2628
76. Hiltunen, M., Lu, A., Thomas, A. V., Romano, D. M., Kim, M., Jones, P. B., Xie, Z., Kounnas, M. Z., Wagner, S. L., Berezovska, O., Hyman, B. T., Tesco, G., Bertram, L., and Tanzi, R. E. (2006) *J. Biol. Chem.* **281,** 32240–32253
77. Harrison, F. E., and May, J. M. (2009) *Free Radic. Biol. Med.* **46,** 719–730
78. Spector, R. (2009) *J. Neurochem.* **111,** 315–320
79. Harrison, F. E., Hosseini, A. H., McDonald, M. P., and May, J. M. (2009) *Pharmacol. Biochem. Behav.* **93,** 443–450
80. Pejler, G., Lindahl, U., Larm, O., Scholander, E., Sandgren, E., and Lundblad, A. (1988) *J. Biol. Chem.* **263,** 5197–5201